PHYSICAL AND ELECTROCHEMICAL PROPERTIES OF BORON – DOPED DIAMOND (BDD) ELECTRODE

Nguyen Tien Hoang

The University of Danang, University of Education; tienhoangedu@gmail.com

Abstract - The physical and electrochemical behaviors of BDD electrode are clarified in this work. The surface morphology of BDD is investigated by scanning electron microscopy (SEM) before and after electrolysis in different conditions. There is not any corrosion found on the surface based on the studies of SEM and electrochemical corrosion process. The contact angle of BDD surface with pure water is changed from hydrophobic to hydrophilic (characterized by 97º and 28º) after several runs. In order to thoroughly investigate chemical composition of BDD, Raman spectroscopy is used. The featured peak of diamond is found at 1332 cm^{-1} Raman shift. The comparison between H-terminated and O-terminated peaks (O 1s and C 1s) as a result of electrochemical processes is made using X-ray photoelectron spectroscopy (XPS). The cyclic voltammogram (CV) of BDD is studied in acid and alkaline media in the range of hydrogen and oxygen evolution.

Key words - Boron doped diamond; electrode; electrochemical properties; the cyclic voltammogram; surface morphology

1. Introduction

Doped diamond electrodes have been applied in electrochemical field since 1983 [1]. The electrochemical properties of boron-doped diamond (BDD) such as wide potential window, the electrochemical stability in both cases (aqueous and non-aqueous solutions), resistance to the adsorption of organic molecules, long term stability with air contact, the wide application for low detection of species were investigated by many authors [2-7]. Diamond in the form of monocrystalline or polycrystaline structure where each atom links with three other sp^3 hybridized carbons as building a tetrahedral bond. To increase the conductivity of diamond, boron is doped onto the surface of diamond to form so-called synthetic boron-doped diamond, where boron acts as an electron acceptor due to an electron deficiency in its external shell [8], [9], and thus the diamond electrodes can perform as p-type semiconductor.

Because of the unique properties, for example, the extreme robustness and high resistance to corrosion, BDD is considered as an excellent electrode material for the anodic oxidation of organic in wastewater treatment application.

Due to the high cost of such electrode, the application in industrial field is still challenging. However, the properties of BDD in laboratory scales have been widely studied, including in the biological treatment field [10]. Organic pollutants can be oxidized directly on BDD electrodes (by electron transfer from surface to compound) and indirectly by the generation of $^{\bullet}OH$ radicals [11] and/or other weaker oxidizing species when oxidizing water. The physical properties of BDD electrodes can be studied by investigating the surface of the deposited diamond layer, layer thickness as well as the surface morphology. For the study of the electrochemical properties, cyclic voltammetry was considered as one of the main investigated parameters.

However, there has been so far a limited number of public papers studying on BDD in Vietnam. The physical and electrochemical properties of BDD have been widely studied for different purposes of use. And thus, it is necessary to specify the physical and electrochemical characterizations of BDD electrode, partly for applying to wastewater treatment [1] based the stability of BDD, high over potential of oxygen and hydrogen and resistance to the corrosion.

2. Experimental section

2.1. Reagents and solutions

All reagents were analytical grade (99% purity). Sufulric acid, phosphoric acid sodium hydroxide, potassium ferri/ ferro-cyanide were acquired from Sigma-Aldrich, whereas ethanol (Merck Co) was used to clean the BDD surface electrode Solutions were prepared using ultrapure water (Seralpur Pro 90 C).

2.2. Experimental details

Bulk electrolysis was carried out at room temperature (22°C) in a 400 mL one-compartment electrochemical cell. BDD electrode (purchased from Neocoat Co, Switzerland) was used as working electrode with 3.8 cm^2 exposed surface area, the thickness of the diamond layer was 2.5 - 3 µm. Platinum foil and Ag/ AgCl (3 M KCl) were used as counter and reference electrodes, respectively. The redox couple $K_3Fe(CN)_6$/ $K_4Fe(CN)_6$ was prepared by adding 200 mL $K_3Fe(CN)_6$ in 0.5 M KOH.

The tested solutions were continuously stirred with a magnetic stirrer bar throughout the process. Before starting the experiments, the BDD electrode was subjected to ultrasonication for 5 min to remove surface contaminants, and then washed with de-ionized ultrapure water. The Pt electrode was washed with de-ionized ultrapure water (Seralpur Pro 90 C).

The electrochemical experiments were performed using IviumStat. Figure 1 describes the setup of one-compartment glass cell and the holder of BDD electrode. The electro-polishing method for BDD was conducted in hard condition of 1 M H_2SO_4 + 3 M H_3PO_4 for 1 h at high current density of j = 2 $A{\cdot}cm^{-2}$.

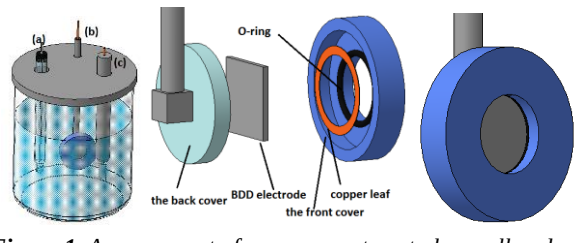

Figure 1. *Arrangement of one-compartment glass cell and the Teflon holder for BDD, (a) reference electrode (Ag/AgCl), (b) BDD electrode, (c) counter electrode (platinum electrode)*

Optical Tensiometer TL 100 was used to determine

static contact angle of water on the surface of BDD. Visualization of the surface was achieved using scanning electron microscopy (SEM). The quality of diamond film was verified using Raman spectroscopy under 514.7 nm excitation. The experiments were conducted in the backscattering geometry using an optical microscope with a high numerical aperture objective (100 X/N.A. 0.9). The laser light was focused on the sample with a power below 1 mW. The Raman scattered light was dispersed using the diffraction grating on a back-illuminated liquid nitrogen-cooled CCD detector.

To generate X-ray source, a mono-chromated Al Kα was used inX-ray photoelectron spectroscopy (XPS) Ulvac Φ 3300 (Ulvac-Phi, Japan). The electron take off angle (the angle between the analyzer and the surface) was 45º after focusing the monochromator radiation on the sample. The pass energy for broad scanning (i.e: C 1s, O 1s and C KLL) was set at 89.5 eV as recommended by many authors. To deconvolve the constituent C 1s peaks and to integrate peak areas, multipack spectrum software (in Origin) is used. The spectra were recorded by in-situ method of the analyzed sample surface in order to avoid any possible variations or contaminations on the surface. The background was firstly subtracted using Shirleys methods and then fitted with the de-convolution of Gaussian and Lorentzian shapes.

3. Results and discussion

3.1. Surface termination

It is important to understand the surface termination of a BDD electrode because it affects: (1) the electron transfer (ET) kinetics of inner sphere redox processes [12] (2) the wetting properties of the electrode, (3) the electrostatic interactions which can result in an increase or decrease of the energy levels in the valence (E_{VB}) and conduction bands (E_{CB}) due to the polarity of the surface bond.

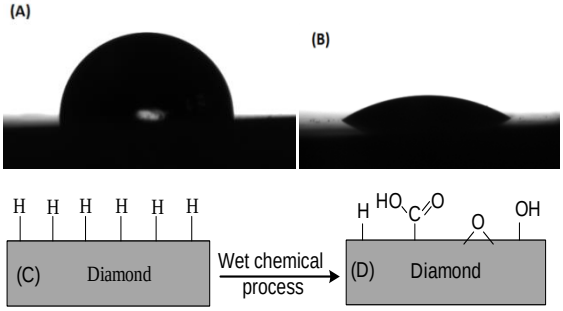

Figure 2. *(a) Contact angle of water with H-terminated BDD surface, (b) contact angle after electrolysis, (c) H-terminated boron doped diamond surface, (d) O-terminated boron doped diamond surface*

As can be seen in Figure 2a, a hydrophobic surface displays water contact angles of 97º between the dropping water and unused electrode. It means that this kind of surface termination (i.e: H-terminated surface $C^{\delta-}$-$H^{\delta+}$) can result in a arise in both of (E_{VB}) and (E_{CB}), and thus creasing the electron transfer between the E_{VB} and H_3O^+ more easily, leading to the increase in the surface conductivity [13]. It is reported that the stability of H-terminated surface can be achieved in air for several months thanks to the low oxidation possibility of its terminated group [8], [14]. After several runs, the BDD surface becomes hydrophilic with the appearance of some oxygenated groups (as seen in Figure 1d) which are detected by XPS. As a result, the contact angle of the surface was measured at about 28º, showing the hydrophilic property after several runs (Figure 2b).

The mechanism of growing H-terminated BDD was achieved in hot filament Chemical vapor deposition process (HFVCD)- one of the effective methods applied by Neocoat Co [15]: The gas mixture containing hydrocarbon (particularly methane/ hydrogen) is introduced into the hot chamber and under hot condition molecular hydrogen (H_2) dissociates into atomic hydrogen due to the activation of hydrogen. Diamond growth took place via site-activation by the surface hydrogen displayed in reaction (1) and then followed by the attack of hydrocarbon radical CH_3 to C_d in reaction (2). Additionally, the recombination reaction of atomic hydrogen can occur as shown in reaction (3):

$$C_dH + H^\bullet \Leftrightarrow C_d^\bullet + H_2 \quad (1)$$

$$C_d^\bullet + CH_3^\bullet \Leftrightarrow C_d\text{-}CH_3 \quad (2)$$

$$C_d^\bullet + H^\bullet \Leftrightarrow C_d\text{-}H \quad (3)$$

3.2. Surface morphology, cross section and Raman microscopy

The morphology of BDD electrode was characterized by SEM with magnifications of 2µm and 500nm presented in Figure 3.a. As seen in this figure, the film consists of many grains with an average grain size of 200nm and the grains are randomly oriented to grow diamond crystallites. Figure 3b shows sharp triangular facets due to exposed (1 1 1) planes. It can be seen clearly in Figure 3.c that the thickness layer of crystal morphology of diamond is about 2.5 µm -3 µm.

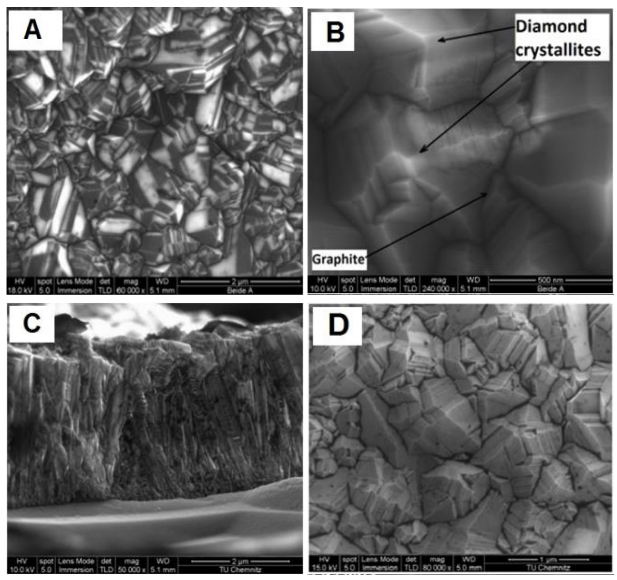

Figure 3. *(a, b) SEM images of BDD electrode surface at 2µm and 500nm resolution respectively, (c) cross section of BDD layer on Si substrate, (d) BDD surface after electro-polishing in 1 M H_2SO_4 + 3M H_3PO_4, T = 50ºC for 1h at current density j = 2 A·cm^{-2}*

In 1 M H_2SO_4 + 3 M H_3PO_4 no corrosion or defect is observed on the surface after 1h of polishing based on SEM observation. The surfaces of BDD in Figure 3b and in Figure 3d are roughly the same. It can be concluded that the BDD is physically stable in hard conditions of treatment.

The Raman spectroscopy analysis only shows the presence of some sp^3 component and sp^2 carbon species although there are various components from the presence of some disorder in diamond as well as other smaller crystals. As can be seen in Figure 4, the significant intensity of high sharp peak of sp^3 vibrates at 1332 cm^{-1} in the Raman spectrum, which was observed similarly by D.S. Knight [16]. The broad bands around 1381 cm^{-1} and 1553 cm^{-1} originating from a sp^2 component suggest that the carbon films also contain another carbon component. The usual G band in graphite with pure sp^2 hybridization shows a band around 1580 cm^{-1} [17]. Here this band shifts to around 1553 cm^{-1} due to the weakening of the C=C bond [13]. The band around 1159 cm^{-1} and 1484 cm^{-1} were attributed to trans-polyacetylene [18].

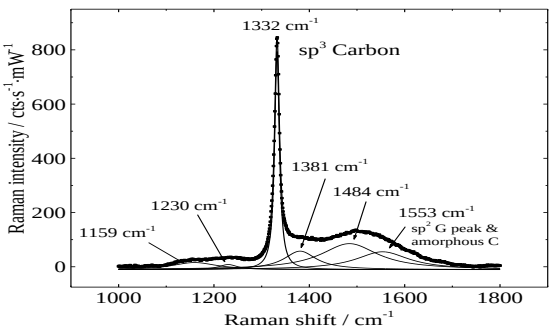

Figure 4. *Raman spectrum from the diamond film acquired under 514.7 nm laser excitation*

3.3. X-ray photoelectron spectroscopy (XPS) and the conversion from hydrogenated to oxygenated surface on diamond

XPS is a sensitive technique for the surface chemistry study. In our investigation, both wide and high resolution XPS spectra were recorded to study the hydrogen, oxygen groups and oxygen-related groups on BDD.

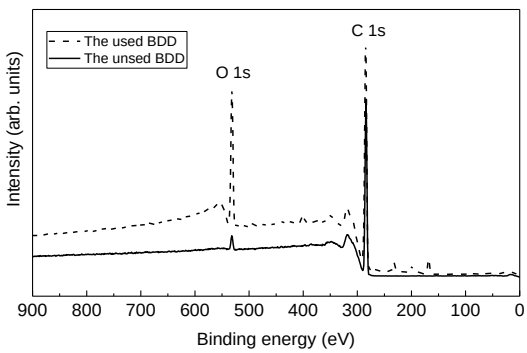

Figure 5. *Wide XPS spectra of the used and unused BDD surface*

In Figure 5, the core-level C 1s peak was found at around 284.2 eV as the highest peak in the arrangement of binding energy, meanwhile the secondary peak which attributes to O 1s peak displays at around 533 eV. The intensity for O 1s on the used BDD is approximately 10 times higher than on the unused one, indicating the oxygen content increased remarkably after several runs It is predictably explained that oxygen chemically and physically absorbed onto the BDD surface during electrolysis. As a result, the surface became hydrophilic.

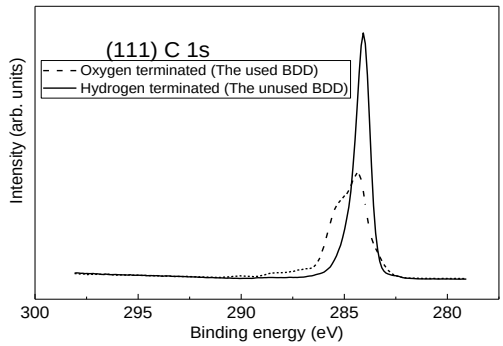

Figure 6. *High resolution of C 1s on the used and unused BDD*

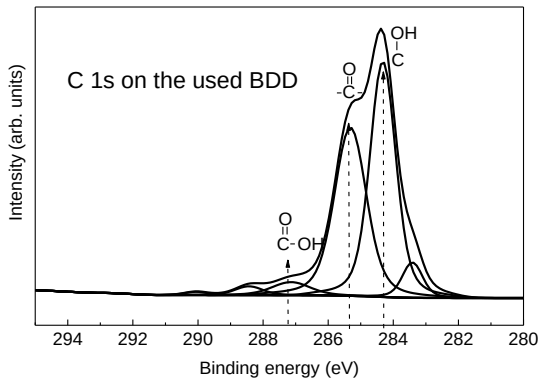

Figure 7. *Oxygen-related components in the used BDD via de-convoluted C 1s*

The core-level C 1s peaks (Figure 6) shows the change between hydrogenated and oxygenated (111) diamond surface. The sharp high intensity for hydrogenated termination C 1s is observed while that for oxygenated termination shows a wider asymmetric tail at similar binding energy.

The C 1s spectra from Figure 6 were then carefully de-convoluted into five peaks as shown in Figure 7 in case of the used BDD. According to the previous study [15], some oxygen terminated groups were identified at the same binding energy: hydroxyl (C–OH) as the main peak of the C 1s core-level displayed at 284.2 eV attributing to the sp^3 hybridized carbon in BDD, carbonyl (C=O) at 285 eV and carboxyl acid (HO–C=O) at 287.2 eV.

3.4. Electrochemical properties in aqueous electrolytes

Cyclic voltammetry of BDD in alkaline and acid media

The main electrochemical behavior of diamond electrodes in aqueous electrolytes has been investigated. The unique property of BDD electrode compared with other ones is a high over-potential for both oxygen and hydrogen evolution [19-21]. Figure 8 shows cyclic voltammograms when testing BDD electrode in 1 M

H_2SO_4 and 1 M NaOH in the region between hydrogen and oxygen evolution. The high over-potential of diamond electrode for both cases (oxygen and hydrogen evolution) is observed in Figure 8, leading to a wide potential window (approx. 4.2 V in H_2SO_4 and 3.7 V in NaOH). As a result, this makes BDD totally special in comparison to other electrode materials such as gold, platinum or mixed metal oxide electrodes, where water is easily converted in the form of H_2 and O_2 gases instead of being oxidized to the •OH radicals as BDD electrode performed in hydrogen and oxygen evolution ranges.

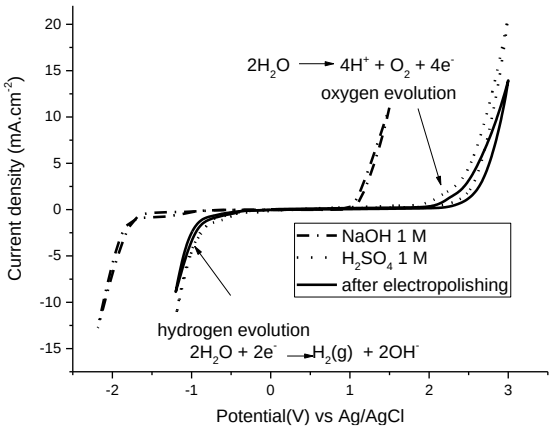

Figure 8. *Cyclic voltammogram of BDD electrode in 1 M H_2SO_4, 1 M NaOH and the CV of BDD in 1M H_2SO_4 after electro-polishing. Scan rate 100 mV·s^{-1}*

The high over-potential of BDD for oxygen evolution tends to oxidize water to •OH radicals as seen an effective oxidizing agent for organics decomposition in wastewater treatment:

$$H_2O \rightarrow OH^{\bullet} + e^- + H^+ \quad (4)$$

High over-potentials on BDD electrodes can be also seen in case of halides (i.e: I^-, Br^-, Cl^-) oxidation [19-21] and in case of the reduction of the corresponding halogens (I_2, Br_2, Cl_2) [22].

Oxygen evolution reaction in water decomposition

The anodic polarization curve for oxygen evolution was recorded in 1 M H_2SO_4 on BDD electrode at the scan rate of 1 mV·s^{-1}. Figure 9 shows the measured polarization curves before and after electro-polishing.

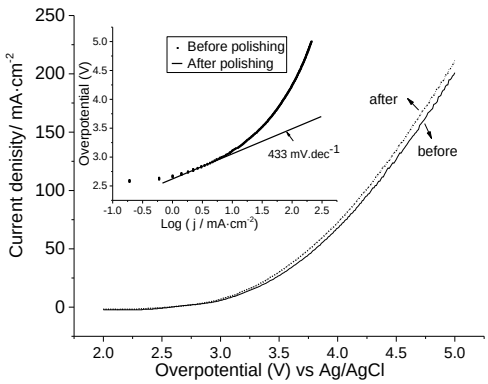

Figure 9. *Current curves over-potential before and after electro-polishing recorded in 1 M H_2SO_4 on BDD electrode at 1 mV·s^{-1}. Insert shows the corresponding Tafel plots*

The oxidation of water to oxygen evolution occurs through electron transfer from a H_2O molecule to the BDD electrode [21] written by the following simplified mechanism:

$$BDD + H_2O \Leftrightarrow BDD\text{-}OH + H^+ + e^- \quad (5)$$

$$BDD\text{-}OH \Leftrightarrow BDD\text{-}O + H^+ + e^- \quad (6)$$

$$2BDD\text{-}O \Leftrightarrow 2BDD + O_2 \quad (7)$$

From both experimental polarization curves, there was no significant difference before and after polishing. Regarding the Tafel lines plotted in the over-potential region > 2.5 V (inset of Figure 9 a high Tafel slope of 433 mV·de^{-1} was obtained. It can be explained that the functional groups on the surface decrease the oxygen evolution reaction (OER) resulting in both high Tafel slope and high over-potentials for oxygen evolution.

The BDD behavior to the redox couple potassium ferri/ ferro-cyanide

The ferri/ ferro-cyanide redox couple is popularly a standard probe thanks to its sensitive possibility for oxidation/ reduction reaction. Figure 10 displays cyclic voltammograms of BDD electrode of the redox couple $K_3Fe(CN)_6$/ $K_4Fe(CN)_6$, showing that the anodic peaks for 0.02 M $K_3Fe(CN)_6$/ $K_4Fe(CN)_6$ corresponding to the oxidation of $K_3Fe(CN)_6$ observed at about 0.42 V. On the other hand, an increase in the concentration of this redox couple causes the deformation of CV sharp due to some reasons: The high concentration of Fe^{3+}/Fe^{2+}, the unclean electrode, the bigger area of counter electrode area compared with working electrode (in our case), the high scan rate, the large distance between working and courter electrodes.

The increase in concentration of potassium ferri/ ferro-cyanide leads to a linear increase in the anodic current magnitude (as shown in Figure 10) with a shift of anodic peak potential by average step of 0.08V.

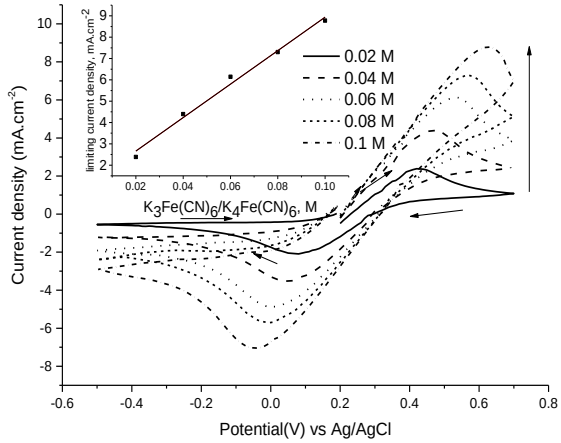

Figure 10. *Current density versus concentration ratio of $K_3Fe(CN)_6$ in 0.5 M NaOH. Supporting electrolyte (0.5 M NaOH) consists of: 0.02M $K_3Fe(CN)_6$ (Solid) 0.04 M (Dash), 0.06 M (Dot), 0.08 M (Short dash), 0.1 M (Short dash dot). Scan rate 100 mV·s^{-1}*

In case of 0.02 M ferri/ferro-cyanide redox couple, the voltage separation between the current peaks $\Delta E_p = |\Delta E_p^{ox} - \Delta E_p^{red}| = 0.4$ V at scan rate of 100 mV·s^{-1}.

ΔE_p shifts towards higher values with increasing its concentration. The CVs response at BDD electrode are found to be very dependent on concentration of ferri/ ferro-cyanide when its concentration is less than 0.1 M.

4. Conclusion

The physical and electrochemical stability of diamond electrode has been investigated in this study. The study of BDD electrode behavior shows that this electrode has a good quality and is stable in both acidic and alkaline conditions at room temperature. Any losses of diamond material of BDD electrode are not found during electrolysis of 1M H_2SO_4, 1M NaOH and electro-polishing in 1M H_2SO_4 + 3M H_3PO_4. It has been considered as one of the major advantages of BDD electrode compared to the conventional electrode materials. However, after several electrolysis processes, the hydrophobic surface of electrode becomes more hydrophilic with presences of some O-terminated groups.

Acknowledgments: This study was supported by Vietnam International Education Development Section, Danang University of Education and Chemnitz University of Technology (Germany). We wish to express our thanks to M. Sommer and E. Dietzsch (Chemnnitz University of Technology) for experimental support and helpful discussions.

REFERENCE

[1] M. Iwaki, S. Sato, K. Takahashi, and H. Sakairi, "Electrical conductivity of nitrogen and argon implanted diamond", *Nucl. Instruments Methods Phys. Res.*, vol. 209–210, no. PART 2, pp. 1129–1133, 1983, doi: 10.1016/0167-5087(83)90930-4.

[2] G. M. Swain and R. Ramesham, "The Electrochemical Activity of Boron-Doped polycrystalline Diamond Thin Film Electrodes", *Anal. Chem.*, vol. 65, no. 4, pp. 345–351, 1993, doi: 10.1021/ac00052a007.

[3] J. Xu, M. C. Granger, Q. Chen, J. W. Strojek, T. E. Lister, and G. M. Swain, "Boron-doped diamond thin-film electrodes", *Anal. Chem.*, vol. 69, no. 19, 1997.

[4] H. B. Martin, "Voltammetry Studies of Single-Crystal and Polycrystalline Diamond Electrodes", *J. Electrochem. Soc.*, vol. 146, no. 8, p. 2959, 1999, doi: 10.1149/1.1392035.

[5] A. Perret *et al.*, "Electrochemical behavior of synthetic diamond thin film electrodes", *Diam. Relat. Mater.*, vol. 8, no. 2–5, pp. 820–823, 1999, doi: 10.1016/s0925-9635(98)00280-5.

[6] H. B. Martin, "Hydrogen and Oxygen Evolution on Boron-Doped Diamond Electrodes", *J. Electrochem. Soc.*, vol. 143, no. 6, p. L133, 1996, doi: 10.1149/1.1836901.

[7] A. Kapałka, G. Fóti, and C. Comninellis, "Determination of the Tafel slope for oxygen evolution on boron-doped diamond electrodes", *Electrochem. commun.*, vol. 10, no. 4, pp. 607–610, 2008, doi: 10.1016/j.elecom.2008.02.003.

[8] E. Vanhove *et al.*, "Stability of H-terminated BDD electrodes: An insight into the influence of the surface preparation", *Phys. Status Solidi Appl. Mater. Sci.*, vol. 204, no. 9, pp. 2931–2939, 2007, doi: 10.1002/pssa.200776340.

[9] T. Kondo *et al.*, "Characterization and electrochemical properties of CF4 plasma-treated boron-doped diamond surfaces", *Diam. Relat. Mater.*, vol. 17, no. 1, pp. 48–54, 2008, doi: 10.1016/j.diamond.2007.10.009.

[10] V. Schmalz, T. Dittmar, D. Haaken, and E. Worch, "Electrochemical disinfection of biologically treated wastewater from small treatment systems by using boron-doped diamond (BDD) electrodes - Contribution for direct reuse of domestic wastewater", *Water Res.*, vol. 43, no. 20, pp. 5260–5266, 2009, doi: 10.1016/j.watres.2009.08.036.

[11] G. Chen, "Electrochemical technologies in wastewater treatment", *Sep. Purif. Technol.*, vol. 38, no. 1, pp. 11–41, 2004, doi: 10.1016/j.seppur.2003.10.006.

[12] A. J. Bard, "Inner-sphere heterogeneous electrode reactions. Electrocatalysis and photocatalysis: The challenge", *J. Am. Chem. Soc.*, vol. 132, no. 22, pp. 7559–7567, 2010, doi: 10.1021/ja101578m.

[13] J. V. Macpherson, "A practical guide to using boron doped diamond in electrochemical research", *Phys. Chem. Chem. Phys.*, vol. 17, no. 5, pp. 2935–2949, 2015, doi: 10.1039/c4cp04022h.

[14] G. R. Salazar-Banda, L. S. Andrade, P. A. P. Nascente, P. S. Pizani, R. C. Rocha-Filho, and L. A. Avaca, "On the changing electrochemical behaviour of boron-doped diamond surfaces with time after cathodic pre-treatments", *Electrochim. Acta*, vol. 51, no. 22, pp. 4612–4619, 2006, doi: 10.1016/j.electacta.2005.12.039.

[15] VCD technologies. Avalaible: https://www.neocoat.ch/en/technology/cvd-technologies

[16] D. S. Knight and W. B. White, "Characterization of diamond films by Raman spectroscopy", *J. Mater. Res.*, vol. 4, no. 2, pp. 385–393, 1989, doi: 10.1557/JMR.1989.0385.

[17] TUINSTRA F and KOENIG JL, "Raman Spectrum of Graphite", *J. Chem. Phys.*, vol. 53, no. 3, pp. 1126–1130, 1970, doi: 10.1063/1.1674108.

[18] A. C. Ferrari and J. Robertson, "Raman spectroscopy of amorphous, nanostructured, diamond-like carbon, and nanodiamond", *Philos. Trans. R. Soc. A Math. Phys. Eng. Sci.*, vol. 362, no. 1824, pp. 2477–2512, 2004, doi: 10.1098/rsta.2004.1452.

[19] M. Panizza and G. Cerisola, "Application of diamond electrodes to electrochemical processes", *Electrochim. Acta*, vol. 51, no. 2, pp. 191–199, 2005, doi: 10.1016/j.electacta.2005.04.023.

[20] M. A. Q. Alfaro, S. Ferro, C. A. Martínez-Huitle, and Y. M. Vong, "Boron doped diamond electrode for the wastewater treatment", *J. Braz. Chem. Soc.*, vol. 17, no. 2, pp. 227–236, 2006, doi: 10.1590/S0103-50532006000200003.

[21] N. Katsuki, "Water Electrolysis Using Diamond Thin-Film Electrodes", *J. Electrochem. Soc.*, vol. 145, no. 7, p. 2358, 1998, doi: 10.1149/1.1838643.

[22] N. Vinokur, "Electrochemical Behavior of Boron-Doped Diamond Electrodes", *J. Electrochem. Soc.*, vol. 143, no. 10, p. L238, 1996, doi: 10.1149/1.1837157.

(The Board of Editors received the paper on 19/2/2020, its review was completed on 20/6/2020)